Atmospheric
Chemistry
and Physics
Discussions

Open Access

European air quality modelled by CAMx including the volatility basis set scheme

G. Ciarelli[1], S. Aksoyoglu[1], M. Crippa[1,a], J. L. Jimenez[2,3], E. Nemitz[4], K. Sellegri[5], M. Äijälä[6], S. Carbone[7,b], C. Mohr[8], C. O'Dowd[9], L. Poulain[10], U. Baltensperger[1], and A. S. H. Prévôt[1]

[1]Paul Scherrer Institute, Laboratory of Atmospheric Chemistry, 5232 Villigen PSI, Switzerland
[2]Cooperative Institute for Research in Environmental Sciences, University of Colorado, Boulder, CO 80309, USA
[3]Department of Chemistry and Biochemistry, University of Colorado, Boulder, CO 80309, USA
[4]Center for Ecology and Hydrology, Bush Estate, Penicuik, Midlothian, EH26 0QB, UK
[5]Laboratoire de Météorologie Physique CNRS UMR6016, Observatoire de Physique du Globe de Clermont-Ferrand, Université Blaise Pascal, 63171 Aubière, France
[6]University of Helsinki, Department of Physics, Helsinki, Finland
[7]Atmospheric Composition Research, Finnish Meteorological Institute, P.O. Box 503, 00101 Helsinki, Finland
[8]Karlsruhe Institute of Technology, Institute of Meteorology and Climate Research, Karlsruhe, Germany
[9]School of Physics and Centre for Climate & Air Pollution Studies, Ryan Institute, National University of Ireland Galway, University Road, Galway, Ireland

Discussion Paper | Discussion Paper | Discussion Paper | Discussion Paper |

ACPD

15, 35645–35691, 2015

European air quality modelled by CAMx

G. Ciarelli et al.

Title Page

Abstract   Introduction

Conclusions   References

Tables   Figures

◀   ▶

◀   ▶

Back   Close

Full Screen / Esc

Printer-friendly Version

Interactive Discussion

[10]Leibniz-Institute for Tropospheric Research (TROPOS), Permoserstr. 15, 04318 Leipzig, Germany

[a]now at: Joint Research Centre, Institute for Environment and Sustainability, 21020 Ispra (Va) JRC, Italy

[b]now at: Institute of Physics, University of São Paulo, Rua do Matão Travessa R, 187, 05508-090 São Paulo, S. P., Brazil

Correspondence to: S. Aksoyoglu (sebnem.aksoyoglu@psi.ch)

Title Page

Abstract	Introduction
Conclusions	References
Tables	Figures

|◄ | ►|

◄ | ►

Back | Close

Full Screen / Esc

Printer-friendly Version

Interactive Discussion

Abstract

Four periods of EMEP (European Monitoring and Evaluation Programme) intensive measurement campaigns (June 2006, January 2007, September–October 2008 and February–March 2009) were modelled using the regional air quality model CAMx with VBS (Volatility Basis Set) approach for the first time in Europe within the framework of the EURODELTA-III model intercomparison exercise. More detailed analysis and sensitivity tests were performed for the period of February–March 2009 and June 2006 to investigate the uncertainties in emissions as well as to improve the modelling of organic aerosols (OA). Model performance for selected gas phase species and $PM_{2.5}$ was evaluated using the European air quality database Airbase. Sulfur dioxide (SO_2) and ozone (O_3) were found to be overestimated for all the four periods with O_3 having the largest mean bias during June 2006 and January–February 2007 periods (8.93 and 12.30 ppb mean biases, respectively). In contrast, nitrogen dioxide (NO_2) and carbon monoxide (CO) were found to be underestimated for all the four periods. CAMx reproduced both total concentrations and monthly variations of $PM_{2.5}$ very well for all the four periods with average biases ranging from –2.13 to 1.04 $\mu g\,m^{-3}$. Comparisons with AMS (Aerosol Mass Spectrometer) measurements at different sites in Europe during February–March 2009, showed that in general the model over-predicts the inorganic aerosol fraction and under-predicts the organic one, such that the good agreement for $PM_{2.5}$ is partly due to compensation of errors. The effect of the choice of volatility basis set scheme (VBS) on OA was investigated as well. Two sensitivity tests with volatility distributions based on previous chamber and ambient measurements data were performed. For February–March 2009 the chamber-case reduced the total OA concentrations by about 43 % on average. On the other hand, a test based on ambient measurement data increased OA concentrations by about 47 % for the same period bringing model and observations into better agreement. Comparison with the AMS data at the rural Swiss site Payerne in June 2006 shows no significant improvement in modelled OA concentration. Further sensitivity tests with increased biogenic

Title Page

Abstract | Introduction

Conclusions | References

Tables | Figures

◄ | ►◄

◄ | ►

Back | Close

Full Screen / Esc

Printer-friendly Version

Interactive Discussion

and anthropogenic emissions suggest that OA in Payerne was largely dominated by residential heating emissions during the February–March 2009 period and by biogenic precursors in June 2006.

1 Introduction

Air pollution is known to cause damage to human health, vegetation and ecosystems. It is one of the main environmental causes of premature death. Only in Europe, more than 400 000 premature deaths were estimated in 2011 with $PM_{2.5}$ (particles less than 2.5 μm in aerodynamic diameter) having the highest relative risk for health damage (WHO, 2014). Air quality models help understanding the processes taking place between emission sources and pollutant concentrations at receptor sites. They are very useful to define control strategies for future legislation. In spite of large improvements in recent years, Chemical Transport Models (CTMs) have still some uncertainties (Solazzo et al., 2012). Various air quality model intercomparison exercises were successfully carried out over the last decades to determine uncertainties in chemical and physical processes governing particulate matter and its precursors (Solazzo et al., 2012; Bessagnet et al., 2014). However, a large variability in particulate matter concentrations was found between different models indicating process parameterization as one of the main reasons for such discrepancies. Moreover, recent studies based on AMS (Aerosol Mass Spectrometer) measurements at different sites in Europe, revealed that the organic fraction dominates the non-refractory PM_1 composition (Crippa et al., 2014). Organic aerosol (OA) can be found in the atmosphere from direct emission by various sources, such as fossil fuel combustion by road vehicle engines or residential wood combustion. Direct emissions of OA are typically referred to as primary organic aerosol (POA) whereas gas-to-particle conversion is referred to as secondary organic aerosol (SOA). Formation mechanisms of SOAs are not very well known yet and their representation in CTMs is still challenging (Hallquist et al., 2009; Fountoukis et al., 2011; Bergstrom et al., 2012; Li et al., 2013; Langmann et al., 2014; Tsigaridis

et al., 2014). In one of our recent aerosol modelling studies we compared model $PM_{2.5}$ prediction with PM_1 AMS measurements for different sites (Payerne and Zürich) and periods (summer and winter) in Switzerland. We found that particulate matter was generally well reproduced by the model with the SOA fraction being under-predicted

5 and POA over-predicted (Aksoyoglu et al., 2011). Traditional CTMs treat POA as non-volatile. Some studies however have revealed the semi-volatile nature of POA, through its dynamic equilibrium of organic aerosol with its gas phase, and the importance of semi-volatile (SVOC) and intermediate volatility (IVOC) organic compounds as SOA precursors (Donahue et al., 2006; Robinson et al., 2007; Cappa and Jimenez, 2010).

10 To describe the absorptive partitioning and ongoing oxidation of the atmospheric material, a volatility basis set (VBS) where organic species are organized into surrogates according to their volatility was developed (Donahue et al., 2011, 2012a, b). Air quality models updated with VBS scheme started being used (Lane et al., 2008; Murphy and Pandis, 2009; Hodzic et al., 2010; Fountoukis et al., 2011; Bergström et al., 2012;

15 Murphy et al., 2012; Jo et al., 2013; Zhang et al., 2013; Athanasopoulou et al., 2013; Fountoukis et al., 2014). Bergström et al. (2012) reported an EMEP model study over Europe for the 2002–2007 period using different assumptions regarding partitioning and aging processes. They could not reproduce the measured OA levels in winter suggesting that residential wood combustion inventories might be underestimated in differ-

20 ent parts of Europe. Fountoukis et al. (2014) applied the PMCAMx model to simulate EUCAARI (Kulmala et al., 2009, 2011) and EMEP (Tørseth et al., 2012) campaigns in Europe. They could reproduce most of PM_1 daily average OA observations within a factor of two, with the February–March 2009 period having the largest discrepancies. Zhang et al. (2013) deployed the CHIMERE model with the VBS framework during the

25 MEGAPOLI summer campaign in the Greater Paris region for July 2009. They found a considerable improvement in predicted SOA concentrations which might be even overestimated depending on the emission inventory used. In our study, we applied the regional air quality model CAMx with the VBS scheme for the first time in Europe within the framework of EURODELTA-III model intercomparison exercise. In addition

to the base case configuration used in the exercise, more sensitivity tests with the VBS scheme for winter and summer episodes were performed together with a general evaluation of the four EMEP field measurement campaigns.

2 Method

2.1 The EURODELTA-III exercise

The EURODELTA-III (EDIII) framework is a European model intercomparison exercise between several modelling teams sharing both efforts and technical knowledge in order to reduce model uncertainties and to improve understanding of the performances. It contributes to the scientific work of the United Nations Economic Commission for Europe (UNECE) Task Force on Measurement and Modelling (TFMM) within the Convention on Long-range Transboundary Air Pollution (CLRTAP). In the first phase of the EDIII exercise, 4 periods of the EMEP field measurement campaigns were chosen in order to evaluate the model results:

– 1 June–30 June 2006

– 8 January–4 February 2007

– 17 September–15 October 2008

– 25 February–26 March 2009

Multiple models were applied on a common domain and driven with the same input data provided by the National Institute for Industrial Environment and Risks (INERIS). However, for some models, different meteorology, boundary conditions and emissions data such as biogenic emissions were used (Bessagnet et al., 2014).

2.2 Modelling method

2.2.1 CAMx

The Comprehensive Air quality Model with extensions, CAMx-VBS (CAMx5.41_VBS, kindly provided by ENVIRON before its public release) was used in this study. The model domain consisted of one grid with a horizontal resolution of $0.25° \times 0.25°$. The latitude and longitude grid extended from $25.125°$ W to $45.125°$ E and 29.875 to $70.125°$ N resulting in 281×161 grid cells covering the whole of Europe. Hourly four-dimensional meteorological fields for wind speed and direction, pressure, temperature, specific humidity, cloud cover and rain required by CAMx simulations were calculated from ECMWF IFS (Integrated Forecast System) data at $0.2°$ resolution. Vertical diffusivity coefficients were estimated following the Kz approach of O'Brien (1970) using PBL depth profiles as available in IFS data. CAMx simulations used 33 terrain-following σ-levels up to about 8000 m a.g.l. No vertical interpolation of the original IFS data was performed. The lowest layer was about 20 m thick. MACC (Monitoring Atmospheric Composition and Climate) reanalysis data were used to initialize initial and the boundary condition fields (Benedetti et al., 2009; Inness et al., 2013). Elemental carbon, organic aerosol, dust and sulfate were used to model aerosol species at the boundaries of the domain. One half of the OA was assumed to be secondary organic aerosol (SOA) and the other half primary organic aerosol (POA), as recommended in the EDIII exercise. Photolysis rate inputs were calculated using the TUV radiative transfer and photolysis model (Madronich, 2002). The required ozone column densities to determine the spatial and temporal variation of the photolysis rates were extracted from TOMS data (http://ozoneaq.gsfc.nasa.gov). Removal processes as dry and wet deposition were simulated using the Zhang resistance model (Zhang et al., 2003) and a scavenging model approach for both gases and aerosols (ENVIRON, 2011), respectively. For the gas phase chemistry the Carbon Bond (CB05) mechanism (Yarwood et al., 2005) with 156 reactions and up to 89 species was used. Partitioning of inorganic aerosols (sulfate, nitrate, ammonium, sodium and chloride) was performed using the

ISORROPIA thermodynamic model (Nenes et al., 1998). Aqueous sulfate and nitrate formation in cloud water was simulated as well using the RADM aqueous chemistry algorithm (Chang et al., 1987).

2.2.2 Emissions

Annual total gridded anthropogenic emissions were prepared and provided by INERIS for the EDIII exercise, which is based on a merging process of data-bases from different sources, i.e. TNO-MACC (Kuenen et al., 2011), EMEP (Vestreng et al., 2007), GAINS (The Greenhouse Gas and Air Pollution Interactions and Synergies). For specific countries where TNO-MACC emissions were missing (Iceland, Liechtenstein, Malta and Asian countries), the EMEP $0.5° \times 0.5°$ emissions were used and re-gridded using adequate proxies such as "artificial land-use" and EPER (European Pollutant Emission Register) data (http://www.eea.europa.eu/) for industries. Total primary particle emissions were made available by EMEP in two different size ranges: below 2.5 µm (fine) and between 2.5 and 10 µm (coarse). Total emissions were later split to estimate the amount of elemental carbon, and organic matter for each of the 10 SNAP codes (Selected Nomenclature for Air Pollution) and country. The final emission inventory thus compiled consisted of 6 gas species namely methane, carbon monoxide, ammonia, sulfur oxides, non-methane volatile organic compounds and nitrogen oxides and 6 categories of particulate matter classes: fine elemental carbon (EC2.5), coarse elemental carbon (EC10), fine primary organic material (fine POA), coarse primary organic material (coarse POA), fine other primary particulate material (non-carbonaceous) and coarse other primary particulate material (non-carbonaceous). Total non-methane volatile organic compounds were split for the CB05 mechanism using the recommendations of Passant (2002). Hourly, weekly and monthly time profiles as in the EURODELTAII exercise were applied to total annual anthropogenic emissions. Biogenic VOC emissions were calculated using the Model of Emissions of Gases and Aerosols from Nature MEGANv2.1 (Guenther et al., 2012). This model is driven by meteorological variables such as hourly temperature, solar radiation, humidity, wind

speed, soil moisture and land cover data including leaf area index (LAI) and plant function type (PFT) as available in the Community Land Model 4.0. 8 days average satellite data at 0.25° × 0.25° resolution were pre-processed and made available from the TERRA/MODIS satellite system. Sixteen plant function types including needle-leaved evergreen, needle-leaved deciduous, broad-leaved evergreen, broad-leaved deciduous, grass and crop for different climatic zones were prepared for this study at 0.25° × 0.25° resolution together with the global emission factors of α-pinene, β-pinene, 3-carene, isoprene, limonene, 232-methylbutenol, myrcene, NO_x, t-β-ocimene and sabinene. Common BVOC species such as isoprene, terpene, sesquiterpene, xylene and toluene were obtained for each hour and cell in the domain.

2.2.3 VBS scheme

A new volatility basis set (VBS) scheme is available in the CAMx model to describe changes in oxidation state and volatility. A total of four basis set simulates the evolution of organic aerosol in the atmosphere (Koo et al., 2014). POA emissions were split in HOA-like and BBOA-like emissions and allocated in two different basis sets. HOA-like emissions include emissions from all SNAP sectors except SNAP2 (non-industrial combustion plants) and SNAP10 (agriculture) which were assigned to BBOA-like emissions. Two other sets were used in the model to allocate secondary organic aerosol from anthropogenic (i.e. xylene and toluene) (ASOA) and biogenic (i.e. isoprene, monoterpene and sesquiterpene) (BSOA) gaseous precursors. These two sets also allocate oxidation products of POA vapours, from each of the two primary sets (HOA-like and BBOA-like). The 2-D volatility space retrieved by Donahue et al. (2011, 2012a, b) was used to distribute the organic molecular structures for each of the volatility bins and different sets (Table S1 in the Supplement). Five volatility bins represent the range of semi-volatile organic compounds (SVOCs) ranging from 10^{-1} to 10^{3} µg m^{-3} in saturation concentrations (C^*). Oxidation processes are modelled by shifting C^* by a factor of 10 in the next lower volatility bin, increasing the oxidation state and reducing the carbon number to account for fragmentation. OH reaction rates are assumed

to be 4×10^{-11} cm^3 molecule^{-1} s^{-1} for the reaction of semi-volatile primary vapors with OH and 2×10^{-11} for further aging of ASOA and POA vapours from HOA-like emissions. More details about the VBS parameterization in CAMx can be found in Koo et al. (2014). Further aging of BSOA is not considered in this study based on previous modelling results showing over-prediction of OA when such process is taken into account (Lane et al., 2008; Murphy and Pandis, 2009). This implies that also further aging of POA vapours from BBOA-like emissions was not considered since it is performed in the same basis set. In this work we focus on the effects of a VBS framework on the total OA fraction. Aging processes and alternative VBS implementations will be discussed together with SOA and POA components in a following paper. Three sensitivity tests were performed with different assumptions on the volatility distributions (Table 1):

– S1: Primary organic aerosol was assumed to be non-volatile. Biogenic (isoprene, monoterpenes and sesquiterpenes) and anthropogenic (xylene, toluene and other aromatics) volatile organic compounds (VOCs) were used as precursors for secondary organic aerosol. Partitioning of condensable gases to secondary organic aerosol was calculated using a semi-volatile equilibrium approach (Strader, 1999).

– S2: Primary organic aerosol was assumed to be volatile and undergo chemical oxidation. The volatility distribution estimated by Robinson et al. (2007) was applied to HOA-like and BBOA-like emissions. Emissions of intermediate volatility organic compounds (IVOCs) were assumed to be 1.5 times those of primary organic aerosol (POA) as suggested by Robinson et al. (2007).

– S3: Primary organic aerosol was assumed to be volatile and undergo chemical oxidation using the approach of Shrivastava et al. (2011) and Tsimpidi et al. (2010). The total primary emissions are roughly 3 times higher than in S2. Different volatility distributions were applied for HOA and BBOA-like emissions. IVOCs were assumed to be 1.5 times the amount of POA. This implies that for this scenario the SVOC + IVOC mass added is equal to 7.5 times the initial amount of POA. This

represents the base case scenario used to evaluate gas phase and PM$_{2.5}$ model performance.

Based on the S3 base case scenario, two other sensitivity tests were performed with respect to emissions:

- S4: Increased BVOCs emissions by a factor of 2.

- S5: Increased BBOA-like emissions by a factor of 2.

2.3 Statistical methods

Statistical procedures as available in the Atmospheric Model Evaluation Tool (AMET, Apple et al., 2010) were used in this study to evaluate model performance. Daily ambient measurements of main gas phase species i.e. O$_3$, NO$_2$, CO, SO$_2$ and fine particulate matter (PM$_{2.5}$) were extracted from the Airbase database in Europe and statistics reported in terms of mean bias (MB), mean error (ME), mean fractional bias (MFB) and mean fractional error (MFE):

$$MB = \frac{1}{n} \sum_{i=1}^{n} (M_i - O_i), \tag{1}$$

$$ME = \frac{1}{n} \sum_{i=1}^{n} (|M_i - O_i|), \tag{2}$$

$$MFB = \frac{2}{n} \sum_{i=1}^{n} \left(\frac{M_i - O_i}{M_i + O_i} \right), \tag{3}$$

$$MFE = \frac{2}{n} \sum_{i=1}^{n} \left(\frac{|M_i - O_i|}{M_i + O_i} \right). \tag{4}$$

where M_i presents the modelled value, O_i the observations and n the total number of data points. Due to the coarse grid resolution, only rural-background stations, defined

as stations far from city sources of air pollution with pollution levels determined by the integrated contribution from all sources upwind of the station (ETC/ACC, 2004), with at least 80 % daily average observations available were considered for the statistical analysis. For $PM_{2.5}$ this results in 48 stations available for June 2006, 56 for January–February 2007, 90 for September–October 2008 and 110 stations for February–March 2009. $PM_{2.5}$ components were further evaluated for the February–March 2009 period where comprehensive high resolution AMS measurements at 11 European sites were available, i.e., at Barcelona, Cabauw, Chilbolton, Helsinki, Hyytiälä, Mace Head, Melpitz, Montseny, Payerne, Puy de Dôme and Vavihill (Crippa et al., 2014).

3 Results and discussions

3.1 Model evaluation

Model performance metrics for gas phase species CO, NO_2, O_3 and SO_2 as well as for $PM_{2.5}$ are reported in Fig. 1 and Table 2 and they refer to the base case S3. SO_2 and O_3 concentrations were found to be over-predicted for all the four periods with a mean fractional bias ranging from 14 to 36 % for SO_2 and from 2 to 48 % for O_3. Both O_3 and SO_2 over-predictions were higher during the January–February 2007 periods. The mean error (ME) in SO_2 concentrations increases at stations located close to coastal areas, especially near large harbors such as Lisbon, Marseille, Barcelona and in Eastern countries of the domain (Fig. S1 in the Supplement). Most of the SO_2 emissions arise from high stack point sources which have injection heights of few hundred meters. It might be that the vertical distribution of SO_2 might affect the model performance in particular near the harbors and coastal areas where ship emissions were allocated in the second layer of the model domain (extending from ~ 20 to 50 m a.g.l.) whereas they can reach up to 58 m in deep draft vessels (SCG, 2004) and also undergo plume rise. On the other hand NO_2 and CO were found to be under-predicted for all the four periods with mean fractional bias between -54 and -28 % for NO_2 and -31 and -11 %

for CO. NO_2 was particularly under-predicted during June 2006 whereas CO had the largest bias during the September–October 2008 simulation. The under-prediction in NO_2 concentrations could be influenced by the relatively coarse resolution of the domain which may result in too low NO_x emissions. Possible positive artefacts in the chemiluminescence methods for measuring NO_2 may also occur when NO_2 is catalytically converted to NO on the molybdenum surface leading to an over-prediction of measured NO_2 concentrations (Steinbacher et al., 2007). Moreover, an evaluation of planetary boundary layer height (PBLH) within the EDIII shows that although the PBLH was quite well represented in general in the ECMWF IFS meteorological fields, CAMx tends to under-estimate the night-time minima and to over-estimate some daytime peaks, whereas the wind speed was relatively well reproduced (Bessagnet et al., 2014). Especially in June 2006, when the photochemical activity is higher, the general under-prediction of NO_x in the whole domain reduces the O_3 titration potential during the night time. Model performance for O_3 is also strongly influenced by long-range transport especially during the winter periods when the local chemical production of O_3 is limited. MACC analysis data at $1.125° \times 1.125°$ were used in this study to map O_3 four-dimensional data at the boundary of the domain. Figure S2 in the Supplement shows the model performance at the Mace Head station located on the west coast of Ireland for all the four periods. Especially in January–February 2007 O_3 concentrations were found to be over-predicted by about 10 to 20 ppb indicating that boundary conditions for O_3 were probably not well represented. In June 2006 and September–October 2008 O_3 was relatively well captured at Mace Head suggesting that the observed positive bias in O_3 concentrations might arise from insufficient NO_x emissions to undergo titration during night time as well as not correctly represented planetary boundary layer dynamics. In February–March 2009 the model tends to under-predict the O_3 concentration at Mace Head and overall the O_3 model performance shows the lowest bias (2 %). Eventually, the under-prediction of O_3 in the boundary condition may counteract the already mentioned deficiencies related to insufficient NO_x emissions. Evaluation of O_3 vertical profiles at stations located near the boundaries of the domain show that

even though the model follows the measured O_3 vertical profiles, it has difficulties to catch the inversion between the low and middle troposphere around 2–3 km a.g.l. with O_3 concentrations under 2 km being over-predicted (Bessagnet et al., 2014). Finally, CO was slightly under-predicted for all periods (mean fractional bias between −11 and −31 %), with highest values during the September–October 2008 period (−31 %). The late summer-fall period is known to be influenced by agricultural open field burning activities which might be missing from standard emission inventories.

Of all investigated variables, CAMx shows the best statistical performance for $PM_{2.5}$. For all four periods the acceptable model performance criteria recommended by Boylan and Russell (2006) for aerosols were met (MFE ≤ +75 and −60 % < MFB < +60 %). The fractional bias ranges from less than 1 % in September–October 2008 up to −13 % in February–March 2009. Also the recommended model performance goals (MFE ≤ +50 and −30 % < MFB < +30 %) were met for all periods except for January 2007. Modelled average $PM_{2.5}$ concentrations are shown in Fig. 2. A different spatial distribution is seen for summer and winter. In June 2006 the model predicts higher concentrations in the southern part of the domain especially over the Mediterranean Sea and North Africa (up to 35 µg m^{-3}). On the other hand, the highest concentrations were predicted in the Po valley area (above 40 µg m^{-3}) and in the southern part of Poland during January–February 2007. During the two colder periods (2007 and 2009) elevated concentrations of around 15 µg m^{-3} are also visible close to urban areas such as Paris and Moscow. Figure 3 shows $PM_{2.5}$ variations at Airbase rural-background sites in terms of medians, 25th and 75th percentiles. In all the four periods CAMx is able to reproduce the observed monthly variation very well with some over-prediction occurring mainly from the 14 to the 17 January 2007 and towards the end of 2008 period. Figure 4 shows $PM_{2.5}$ comparisons in terms of daily average scatterplots. CAMx is able to capture the concentration differences between the four periods with lower peak concentrations of around 40 µg m^{-3} in June 2006 and several high pollution events with concentrations around 60–70 µg m^{-3} for the other periods. For some days in January–February 2007 CAMx strongly over-predicts $PM_{2.5}$ with predicted concen-

European air quality modelled by CAMx

G. Ciarelli et al.

Title Page

Abstract	Introduction
Conclusions	References
Tables	Figures

◄◄	►►
◄	►
Back	Close

Full Screen / Esc

Printer-friendly Version

Interactive Discussion

trations around $100 \, \mu g \, m^{-3}$. The latter occurs mainly at one station located in Italy i.e. Casirate d'Adda (Airbase code IT1464A) with the highest over-prediction on the 17 January. During the 7 and 8 March 2009 CAMx strongly under-predicts at the EMEP stations of Ayia Marina in Cypro (Airbase code CY0002R), most likely due to a Saharan dust event not captured by the model (Fig. S3 in the Supplement). A similar situation was found at Viznar in Southern Spain (Airbase code ES0007R) on the 11 and 12 October 2008 with observed $PM_{2.5}$ concentration above $100 \, \mu g \, m^{-3}$. This time CAMx was able to capture the Saharan dust episode but not its magnitude (Fig. S3).

3.2 Detailed evaluation of $PM_{2.5}$ components in February–March 2009

The modelled concentrations of non-refractory $PM_{2.5}$ components were compared against aerosol mass spectrometer measurements at eleven European sites for the February–March 2009 period (Crippa et al., 2014). Even though the AMS measures particles with a diameter $D < 1 \, \mu m$, the difference between the non-refractory PM_1 and total $PM_{2.5}$ mass is in general rather small as shown in Aksoyoglu et al. (2011), at least for situations without exceedingly high air pollution and situations when sea salt makes large relative contribution to $PM_{2.5}$. The modelled average total non-refractory $PM_{2.5}$ (sum of nitrate, sulfate, ammonium and OA) concentrations match the measurements quite well with a few exceptions (Fig. 5 and Table 3). The model is able to reproduce both high concentrations observed at the urban site Barcelona and low ones at remote sites like Hyytiälä, Finland. Concentrations of inorganic aerosols are over-predicted and OA are under-predicted at most of the stations. Very similar results were also presented by other recent studies (Knote et al., 2011). The effect of different schemes to treat OA is discussed in Sect. 3.3. At the Cabauw site nitrate was the most dominant species (Mensah et al., 2012). Especially at this site the model strongly over-predicts in particular the nitrate (NO_3^-) fraction (by a factor of 3). This site is located in a high NH_3 and NO_x emission area. Emissions of NH_3 mainly arise from agricultural activities and just a minor fraction from the transportation sectors. Figure S4 in the

Printer-friendly Version

Interactive Discussion

Supplement shows the seasonal distribution of the annual NH_3 emissions from agriculture, as provided in the EDIII exercise for Switzerland. High NH_3 emissions are therefore expected in March–April. A comparison with ammonia measurements (available at http://www.bafu.admin.ch/luft/00585/10770/index.html?lang=de) at the Payerne site revealed that the model predicts ammonia reasonably well in June 2006 but that there is a significant overestimation in March 2009 suggesting that the modelled emissions might be too high in spring (Table S2 in the Supplement). A sensitivity test with 50 % reduction in ammonia emissions significantly improved the modelled NO_3^- concentrations at almost all sites (Table S3 in the Supplement). The lowest effect was found at Payerne, in Switzerland where reducing ammonia emissions by half led to a decrease in NO_3^- by about 12 %. These results are in line with previous studies suggesting that aerosol formation during winter is more sensitive to NH_3 emissions in most of Europe whereas in the Swiss Plateau it is more limited by NO_x emissions (Aksoyoglu et al., 2011). Indeed, other potential reasons for the over-prediction of NO_3^- could be related to uncertainties in removal process of HNO_3 as well as dry deposition velocity of NH_3. Substantial over-predictions were found at the higher altitude site of Montseny and Puy de Dôme when compared with first model layer concentrations (ca. 200 and 800 m a.s.l. respectively at these sites). These sites located at about 720 and 1465 m a.s.l., are sometimes not within the PBLH during winter periods. At the Montseny site, the relatively coarse resolution of the model could also influence model performance since the site is located in a complex area about 50 km north-east of Barcelona (Pandolfi et al., 2014). Sulfate concentrations (SO_4^{2-}) were over-predicted at almost all sites and especially at Mace Head suggesting that long-range transport of SO_4^{2-} might be positively biased. Modelled and observed hourly concentrations of NO_3^-, SO_4^{2-}, ammonium (NH_4^+) and OA at Payerne are reported in Fig. 6 for March 2009. The period was characterized by south-westerly winds until the 15 March, north-easterly winds between the 15 and 24 March, and again by south-westerly winds until the end of the simulation (Fig. S5 in the Supplement). Temperature was rarely above 10 °C during day-time and mostly around or slightly below 0 °C at night, with higher temperatures

observed between the 15 and 20 March. Specific humidity was between about 4 and $5\,g\,kg^{-1}$. Low wind speeds (below $2\,m\,s^{-1}$) were observed during the first part of the simulation and higher values exceeding $6\,m\,s^{-1}$ around the 9 March and throughout the end of the simulation. The model was able to reproduce the meteorological parameters very well for most of the time. The temperature was slightly under-predicted at both night and day-times (with a maximum of $-2\,^\circ C$) whereas both the monthly variation and the absolute values of wind speed and specific humidity were reproduced well with a few under-predictions of high wind-speed (6 and 11 March and towards the end of the simulation). The model was able to capture the three NO_3^- and NH_4^- peaks observed around the 7, 18 and 23 March with a general slight over-prediction throughout the whole period. Indeed, the under-prediction in temperature during day and night time could partially explain the over-prediction of the NO_3^- fraction with more NO_3^- partitioning to the aerosol phase which also apply to the other stations used in this study. An evaluation of modelled temperature at the European scale for the February–March 2009 period confirmed that the model systematically under-predicted the 2 m surface temperature (Bessagnet et al., 2014). All the inorganic components were over-predicted during the first four days of March 2009 with a peak around the 3 March. The modelled (PBLH) is reported in Fig. S6 in the Supplement together with the convective boundary layer (CBL) height estimated from Payerne sounding data. The model exhibits very low PBLH during the night until the 5 March. In contrast, from the 5 March until the 11 March PBLH at night was relatively higher, around a few hundred meters. At the same time the NO_3^- concentration was reproduced more closely, with the peak around 7 March being under-estimated. From the 12 until the 19 March the modelled PBLH again showed very low values at night with the NO_3^- concentration being slightly over-predicted. This might suggests that a too shallow PBLH at night could be the reason for such over-prediction. Although the temporal variation was captured, concentrations of OA were under-predicted throughout all the simulation (4.1 and $1.8\,\mu g\,m^{-3}$ observed and modelled average concentrations). Analysis of the OA fraction is discussed in the next section.

Full Screen / Esc

Printer-friendly Version

Interactive Discussion

3.3 Organic aerosols

3.3.1 Sensitivity of OA to the VBS scheme

In this section, effects of different parameterizations of the organic aerosol module on the modelled OA concentrations are discussed. The scatter plots in Fig. 7 show a comparison of daily average OA concentrations against the same AMS measurements as in Table 3 during February–March 2009. Statistics for each scenario are reported in Table 4. When the semi-volatile dynamics of primary organic aerosol is not taken into account (scenario S1), the model under-predicts OA concentrations (MFB: −66 %) with an observed and modelled average concentrations of 2.96 and 1.18 μg m^{-3} respectively. In the S2 scenario POA emissions are allowed to evaporate following the volatility distribution proposed by Robinson et al. (2007) and to undergo chemical oxidation. In this case modelled OA concentrations decrease by about 43 % with respect to S1, predicting an average OA concentration of 0.67 μg m^{-3}. On the other hand, the S3 scenario improves the OA model performance increasing the OA concentrations by about 47 % with respect to S1. Predicted OA concentrations are found to be 1.73 μg m^{-3} on average (MFB: −47 %). Similar behavior during winter periods was also shown in recent studies where the same VBS scheme was applied in the US domain (Koo et al., 2014). Figure 8 shows the modelled total OA concentration over Europe using S1, S2 and S3 scenarios. The model predicts high OA values in the Eastern part of the domain as well as over Portugal, France and the Po Valley (S3). Some hot-spots around large urban areas are also visible, i.e., Paris and Moscow. Higher OA concentrations in the southern part of the domain are observed in the S3 case, likely because of higher temperature and more OH radicals available in that part of the domain leading to an increase in the total organic mass upon reaction with organic vapours. This is in line with the results of Fountoukis et al. (2014) for the February–March 2009 period even though their study predicts lower concentration over the Po valley. Even though model input data and parameterizations are not the same, the S3 case in particularly, uses a very similar volatility distribution as in Fountoukis et al. (2014). Our study predicts

relatively lower OA concentrations (MFB: −0.47, MFE: 0.79) compared to those reported by Fountoukis et al. (2014) (MFB: 0.02, MFE: 0.68) for February–March 2009. Unlike Fountoukis et al. (2014) our study does not include fire emissions and marine organic aerosol which may partially explain the differences. Figure 9 shows hourly modelled and observed OA concentration at Payerne for March 2009 and June 2006. In March 2009 S2 results are lower than those in S1 whereas OA concentrations in S3 case are higher (see Fig. S8 and Table S4 in the Supplement for average concentrations and statistics). In June 2006, the OA mass in S2 is lower than those in S1 while S3 predicts similar concentrations as the S1 scenario (2.43 and 2.56 $\mu g\,m^{-3}$, respectively, Fig. S9 and Table S5 in the Supplement). It has to be noted that the S1 scenario predicts slightly lower OA concentration for June 2006 in Payerne with respect to our previous application (Aksoyoglu et al., 2011), mainly because of a different biogenic model being used which yields lower monoterpene and sesquiterpene emissions. Since both BVOCs and BBOA-like emissions are highly uncertain, sensitivity tests with increased biogenic and anthropogenic emissions were performed and results discussed in the next section (Sect. 3.3.2).

3.3.2 Sensitivity of OA to BBOA-like and BVOC emissions

Emissions of BVOCs compounds (i.e. monoterpenes, isoprene and sesquiterpenes) were doubled in scenario S4, whilst primary organic aerosol emissions from SNAP2 and SNAP10 (BBOA-like) were doubled in scenarios S5, with other emissions and processes represented as in S3. Figure 10 shows modelled and observed OA daily average concentrations for the S3, S4 and S5 scenarios across the sites. Statistics for each scenario are reported in Table 5. Increasing biogenic emissions by a factor of two during February–March 2009 resulted in almost no change in the predicted total OA (1.73 and 1.78 $\mu g\,m^{-3}$ for the S3 and S4 scenarios, respectively). On the other hand, doubling the BBOA-like emissions (S5) during the same period strongly increased the predicted OA mass (up to 2.84 $\mu g\,m^{-3}$ on average). As a result the mean fractional bias decreased further, from −47 to −12 % averaged across the sites. This could eventually

confirm other studies where substantial under-predictions in residential wood burning emissions were underlined (e.g., Bergström et al., 2012). A few points above the 2 : 1 lines in S5 mainly belong to the sites of Montseny, Puy de Dôme and Helsinki. During winter periods, it is likely that elevated stations such Montseny and Puy de Dôme are most of the time above the PBLH, as suggested by previous studies for Puy de Dôme (Freney et al., 2011), whereas model concentrations are extracted from the first layer of the model. In Helsinki, BBOA emissions seem to be overestimated or the dispersion underestimated in the model.

Comparison with a warmer period in June 2006 is reported as well for Payerne where AMS measurements were also available (Fig. 11). In February–March 2009 increasing BBOA-like emissions (S5) reduced the fractional bias from −85 % in S3 to −37 % (Table S4) with an over-prediction occurring during 1–5 of March (Fig. 11, upper panel). As already discussed in Sect. 3.2, it is likely that the vertical mixing processes were not correctly represented by the model since also the inorganic components were over-predicted for the same period. Almost no change in the predicted OA mass was found when biogenic emissions were doubled (scenario S4) (Fig. 11, upper panel) due to lower BVOCs emission during winter periods. Increasing BVOCs emissions in June 2006 increased the predicted OA mass at Payerne site especially during the 12–16 June and towards the end of the simulation period, where higher concentrations and temperature (Fig. S7 in the Supplement) were also observed (Fig. 11, lower panel). In contrast, similar OA concentrations were predicted in Payerne for S3 and S5 during June 2006 (with averages of 2.43 and 2.75 μg m^{-3} respectively). This is in line with a very recent source apportionment study based on ACSM (aerosol chemical speciation monitor) measurements performed in Zürich for 13 months (February 2011– February 2012) which revealed substantial differences between the winter (February– March) and summer (June–August) f_{44}/f_{43} space (organic mass fraction measured at mass to charge ratio 44 and 43) indicating that summer OOA (oxygenated organic aerosol) is strongly influenced by biogenic emission and winter OOA by biomass burning emission (Canonaco et al., 2015). Increased OA concentrations at Payerne

in June 2006 with increased biogenic emissions were also found in other modelling studies. Bergström et al. (2012) used the VBS framework with different assumptions regarding aging processes and compared the model results for June 2006 with the AMS results at Payerne. In their study the total OA was found to be under-predicted with lower bias observed when aging processes were taken into account and biogenic emissions were increased by a factor of 3. Even though their model differs from ours in various aspects (number of volatility bins, aging processes parameterization and input data) in two of their scenario without aging of biogenic SOA Bergström et al. (2012) predicted an average OA concentration ranging from 2.6 to 3.4 $\mu g\,m^{-3}$ which is similar to our base case S3 and S4 scenario (2.43 and 3.4 $\mu g\,m^{-3}$, respectively, Table S5).

4   Conclusions

A modelling study using the regional air quality model CAMx with VBS (Volatility Basis Set) scheme was performed for the first time in Europe within the EURODELTA-III model intercomparison exercise. An evaluation for the main gas phase species and $PM_{2.5}$ for four different periods was performed using the European air quality database Airbase as well as AMS (Aerosol Mass Spectrometer) measurements. The period in February–March 2009 was further analyzed in more detail using different assumptions regarding the volatility of emitted organic aerosol and emissions of precursor. The main findings of this study are summarized below:

- Total $PM_{2.5}$ was modelled very well. The concentration gradients between the four investigated episodes were captured by the model. A few episodes of over-prediction for $PM_{2.5}$ were found in the Po valley region. Some days with high $PM_{2.5}$ loads for stations close to the southern border of the domain were not captured by the model, probably because of missing representation of Saharan dust events.

- In general, for all the four periods, the model under-predicted NO_2 and CO concentrations especially during winter periods likely because of insufficient emis-

sions. On the other hand, O_3 was found to be over-predicted likely because of insufficient NO_x to undergo titration during night-time chemistry or not well captured vertical mixing processes and concentrations at the boundaries. SO_2 was over-predicted especially near coastal areas, presumably mainly because of uncertainties in ships stack height representation in the model, and in the eastern part of the domain where larger emissions are occurring.

– Comparisons with AMS measurements for the February–March 2009 period suggested that the model is able to capture the total non-refractory PM_1 mass. However, the inorganic fraction, especially NO_3^-, being over-predicted and the OA under-predicted. Sensitivity tests with reduced NH_3 emissions generally reduced the positive bias in NO_3^- suggesting potential uncertainties in NH_3 emissions and their seasonal variability.

– Including evaporation and oxidation processes of primary organic particles with the volatility distribution proposed by Robinson et al. (2007) lowered the modelled OA mass both in winter and summer periods. On the other hand, the adjustment of the scheme by Robinson et al. (2007) suggested by Shrivastava et al. (2011) and Tsimpidi et al. (2010) brings model and observation into better agreement by reducing the negative bias for OA by about 29 % (MFB) in winter.

– Sensitivity tests with increased BVOCs and BBOA-like emissions suggested that emissions from residential heating represent an important contributor to total OA during winter periods (February–March 2009). The model under-predicted the winter OA concentrations (MFB −47 % for base case S3) more than gas phase pollutants e.g. NO_2 (Table 2). Eventually, increasing BBOA-like emissions by a factor of 2 brought model and observation to a reasonably good agreement even though the model still under-predicts the OA fraction (−12 % MFB). This underlines the necessity to better constrain emission inventories with a focus on residential heating. Also the implementation of the VBS scheme for domestic wood

burning, which substantially influences both the primary and secondary organic aerosol, should be evaluated.

– A summer period was simulated as well and results were compared at Payerne. In June 2006, the current VBS implementation could not explain the discrepancy between modelled and observed OA. During this period the difference between the model and measurements is likely to be related to BVOCs emissions which are uncertain and difficult to constrain with measurements. In this case the model was sensitive to an increase in biogenic emissions especially during periods with higher temperature and OA concentrations. The latter could confirm the importance of BVOC precursors in summer in Payerne and the way to correctly represent their evolution in the atmosphere.

The Supplement related to this article is available online at doi:10.5194/acpd-15-35645-2015-supplement.

References

Aksoyoglu, S., Keller, J., Barmpadimos, I., Oderbolz, D., Lanz, V. A., Prévôt, A. S. H., and Baltensperger, U.: Aerosol modelling in Europe with a focus on Switzerland during summer and winter episodes, Atmos. Chem. Phys., 11, 7355–7373, doi:10.5194/acp-11-7355-2011, 2011.

Appel, K. W., Gilliam, R. C., Davis, N., Zubrow, A., and Howard, S. C.: Overview of the Atmospheric Model Evaluation Tool (AMET) v1.1 for evaluating meteorological and air quality models, Environ. Modell. Softw., 26, 434–443, 2011.

Athanasopoulou, E., Vogel, H., Vogel, B., Tsimpidi, A. P., Pandis, S. N., Knote, C., and Fountoukis, C.: Modeling the meteorological and chemical effects of secondary organic aerosols during an EUCAARI campaign, Atmos. Chem. Phys., 13, 625–645, doi:10.5194/acp-13-625-2013, 2013.

Benedetti, A., Morcrette, J.-J., Boucher, O., Dethof, A., Engelen, R. J., Fisher, M., Flentje, H., Huneeus, N., Jones, L., Kaiser, J. W., Kinne, S., Mangold, A., Razinger, M., Simmons, A. J., and Suttie, M.: Aerosol analysis and forecast in the European Centre for Medium-Range Weather Forecasts Integrated Forecast System: 2. data assimilation, J. Geophys. Res., 114, D13205, doi:10.1029/2008JD011115, 2009.

Bergström, R., Denier van der Gon, H. A. C., Prévôt, A. S. H., Yttri, K. E., and Simpson, D.: Modelling of organic aerosols over Europe (2002–2007) using a volatility basis set (VBS) framework: application of different assumptions regarding the formation of secondary organic aerosol, Atmos. Chem. Phys., 12, 8499–8527, doi:10.5194/acp-12-8499-2012, 2012.

Bessagnet, B., Colette, A., Meleux, F., Rouïl, L., Ung, A., Favez, O., Cuvelier, C., Thunis, P., Tsyro, S., Stern, R., Manders, A., Kranenburg, R., Aulinger, A., Bieser, J., Mircea, M., Briganti, G., Cappelletti, A., Calori, G., Finardi, S., Silibello, C., Ciarelli, G., Aksoyoglu, S., Prévôt, A., Pay, M.-T., Baldasano, J. M., García Vivanco, M., Garrido, J. L., Palomino, I., Martín, F., Pirovano, G., Roberts, P., Gonzalez, L., White, L., Menut, L., Dupont, J. C., Carnevale, C., and Pederzoli, A.: The EURODELTA III exercise "Model evaluation with observations issued from the 2009 EMEP intensive period and standard measurements in Feb/Mar 2009", MSC-W Technical Report, Oslo, Norway, 2014.

Boylan, J. W. and Russell, A. G.: PM and light extinction model performance metrics, goals, and criteria for three-dimensional air quality models, Atmos. Environ., 40, 4946–4959, 2006.

European air quality modelled by CAMx

G. Ciarelli et al.

Canonaco, F., Slowik, J. G., Baltensperger, U., and Prévôt, A. S. H.: Seasonal differences in oxygenated organic aerosol composition: implications for emissions sources and factor analysis, Atmos. Chem. Phys., 15, 6993–7002, doi:10.5194/acp-15-6993-2015, 2015.

Cappa, C. D. and Jimenez, J. L.: Quantitative estimates of the volatility of ambient organic aerosol, Atmos. Chem. Phys., 10, 5409–5424, doi:10.5194/acp-10-5409-2010, 2010.

Chang, J. S., Brost, R. A., Isaksen, I. S. A., Madronich, S., Middleton, P., Stockwell, W. R., and Walcek, C. J.: A three-dimensional eulerian acid deposition model: physical concepts and formulation, J. Geophys. Res., 92, 14681–14700, 1987.

Crippa, M., Canonaco, F., Lanz, V. A., Äijälä, M., Allan, J. D., Carbone, S., Capes, G., Ceburnis, D., Dall'Osto, M., Day, D. A., DeCarlo, P. F., Ehn, M., Eriksson, A., Freney, E., Hildebrandt Ruiz, L., Hillamo, R., Jimenez, J. L., Junninen, H., Kiendler-Scharr, A., Kortelainen, A.-M., Kulmala, M., Laaksonen, A., Mensah, A. A., Mohr, C., Nemitz, E., O'Dowd, C., Ovadnevaite, J., Pandis, S. N., Petäjä, T., Poulain, L., Saarikoski, S., Sellegri, K., Swietlicki, E., Tiitta, P., Worsnop, D. R., Baltensperger, U., and Prévôt, A. S. H.: Organic aerosol components derived from 25 AMS data sets across Europe using a consistent ME-2 based source apportionment approach, Atmos. Chem. Phys., 14, 6159–6176, doi:10.5194/acp-14-6159-2014, 2014.

Donahue, N., Robinson, A., Stanier, C., and Pandis, S.: Coupled partitioning, dilution, and chemical aging of semivolatile organics, Environ. Sci. Technol., 40, 2635–2643, 2006.

Donahue, N. M., Epstein, S. A., Pandis, S. N., and Robinson, A. L.: A two-dimensional volatility basis set: 1. organic-aerosol mixing thermodynamics, Atmos. Chem. Phys., 11, 3303–3318, doi:10.5194/acp-11-3303-2011, 2011.

Donahue, N. M., Henry, K. M., Mentel, T. F., Kiendler-Scharr, A., Spindler, C., Bohn, B., Brauers, T., Dorn, H. P., Fuchs, H., Tillmann, R., Wahner, A., Saathoff, H., Naumann, K. H., Mohler, O., Leisner, T., Muller, L., Reinnig, M. C., Hoffmann, T., Salo, K., Hallquist, M., Frosch, M., Bilde, M., Tritscher, T., Barmet, P., Praplan, A. P., DeCarlo, P. F., Dommen, J., Prevot, A. S. H., and Baltensperger, U.: Aging of biogenic secondary organic aerosol via gas-phase OH radical reactions, P. Natl. Acad. Sci. USA, 109, 13503–13508, doi:10.1073/pnas.1115186109, 2012a.

Donahue, N. M., Kroll, J. H., Pandis, S. N., and Robinson, A. L.: A two-dimensional volatility basis set – Part 2: Diagnostics of organic-aerosol evolution, Atmos. Chem. Phys., 12, 615–634, doi:10.5194/acp-12-615-2012, 2012b.

Environ: User's Guide, Comprehensive Air Quality Model with Extensions (CAMx), Version 5.40, Environ International Corporation, Novato, California, USA, 2011.

ETC/ACC: Improvement of classifications European monitoring stations for AirBase – a quality control, Technical Paper 2004/7, Bilthoven, the Netherlands, 2004.

Fountoukis, C., Racherla, P. N., Denier van der Gon, H. A. C., Polymeneas, P., Charalampidis, P. E., Pilinis, C., Wiedensohler, A., Dall'Osto, M., O'Dowd, C., and Pandis, S. N.: Evaluation of a three-dimensional chemical transport model (PMCAMx) in the European domain during the EUCAARI May 2008 campaign, Atmos. Chem. Phys., 11, 10331–10347, doi:10.5194/acp-11-10331-2011, 2011.

Fountoukis, C., Megaritis, A. G., Skyllakou, K., Charalampidis, P. E., Pilinis, C., Denier van der Gon, H. A. C., Crippa, M., Canonaco, F., Mohr, C., Prévôt, A. S. H., Allan, J. D., Poulain, L., Petäjä, T., Tiitta, P., Carbone, S., Kiendler-Scharr, A., Nemitz, E., O'Dowd, C., Swietlicki, E., and Pandis, S. N.: Organic aerosol concentration and composition over Europe: insights from comparison of regional model predictions with aerosol mass spectrometer factor analysis, Atmos. Chem. Phys., 14, 9061–9076, doi:10.5194/acp-14-9061-2014, 2014.

Freney, E. J., Sellegri, K., Canonaco, F., Boulon, J., Hervo, M., Weigel, R., Pichon, J. M., Colomb, A., Prévôt, A. S. H., and Laj, P.: Seasonal variations in aerosol particle composition at the puy-de-Dôme research station in France, Atmos. Chem. Phys., 11, 13047–13059, doi:10.5194/acp-11-13047-2011, 2011.

Guenther, A. B., Jiang, X., Heald, C. L., Sakulyanontvittaya, T., Duhl, T., Emmons, L. K., and Wang, X.: The Model of Emissions of Gases and Aerosols from Nature version 2.1 (MEGAN2.1): an extended and updated framework for modeling biogenic emissions, Geosci. Model Dev., 5, 1471–1492, doi:10.5194/gmd-5-1471-2012, 2012.

Hallquist, M., Wenger, J. C., Baltensperger, U., Rudich, Y., Simpson, D., Claeys, M., Dommen, J., Donahue, N. M., George, C., Goldstein, A. H., Hamilton, J. F., Herrmann, H., Hoffmann, T., Iinuma, Y., Jang, M., Jenkin, M. E., Jimenez, J. L., Kiendler-Scharr, A., Maenhaut, W., McFiggans, G., Mentel, Th. F., Monod, A., Prévôt, A. S. H., Seinfeld, J. H., Surratt, J. D., Szmigielski, R., and Wildt, J.: The formation, properties and impact of secondary organic aerosol: current and emerging issues, Atmos. Chem. Phys., 9, 5155–5236, doi:10.5194/acp-9-5155-2009, 2009.

Hodzic, A., Jimenez, J. L., Madronich, S., Canagaratna, M. R., DeCarlo, P. F., Kleinman, L., and Fast, J.: Modeling organic aerosols in a megacity: potential contribution of semi-volatile and

intermediate volatility primary organic compounds to secondary organic aerosol formation, Atmos. Chem. Phys., 10, 5491–5514, doi:10.5194/acp-10-5491-2010, 2010.

Inness, A., Baier, F., Benedetti, A., Bouarar, I., Chabrillat, S., Clark, H., Clerbaux, C., Coheur, P., Engelen, R. J., Errera, Q., Flemming, J., George, M., Granier, C., Hadji-Lazaro, J., Huijnen, V., Hurtmans, D., Jones, L., Kaiser, J. W., Kapsomenakis, J., Lefever, K., Leitão, J., Razinger, M., Richter, A., Schultz, M. G., Simmons, A. J., Suttie, M., Stein, O., Thépaut, J.-N., Thouret, V., Vrekoussis, M., Zerefos, C., and the MACC team: The MACC reanalysis: an 8 yr data set of atmospheric composition, Atmos. Chem. Phys., 13, 4073–4109, doi:10.5194/acp-13-4073-2013, 2013.

Jo, D. S., Park, R. J., Kim, M. J., and Spracklen, D. V.: Effects of chemical aging on global secondary organic aerosol using the volatility basis set approach, Atmos. Environ., 81, 230–244, doi:10.1016/j.atmosenv.2013.08.055, 2013.

Knote, C., Brunner, D., Vogel, H., Allan, J., Asmi, A., Äijälä, M., Carbone, S., van der Gon, H. D., Jimenez, J. L., Kiendler-Scharr, A., Mohr, C., Poulain, L., Prévôt, A. S. H., Swietlicki, E., and Vogel, B.: Towards an online-coupled chemistry-climate model: evaluation of trace gases and aerosols in COSMO-ART, Geosci. Model Dev., 4, 1077–1102, doi:10.5194/gmd-4-1077-2011, 2011.

Koo, B., Knipping, E., and Yarwood, G.: 1.5-Dimensional volatility basis set approach for modeling organic aerosol in CAMx and CMAQ, Atmos. Environ., 95, 158–164, 2014.

Kuenen, J. J. P., Denier van der Gon, H. A. C., Visschedijk, A., Van der Brugh, H., and Van Gijlswijk, R.: MACC European emission inventory for the years 2003–2007, TNO report TNO-060-UT-2011-00588, TNO, Utrecht, the Netherlands, 2011.

Kulmala, M., Asmi, A., Lappalainen, H. K., Carslaw, K. S., Pöschl, U., Baltensperger, U., Hov, Ø., Brenquier, J.-L., Pandis, S. N., Facchini, M. C., Hansson, H.-C., Wiedensohler, A., and O'Dowd, C. D.: Introduction: European Integrated Project on Aerosol Cloud Climate and Air Quality interactions (EUCAARI) – integrating aerosol research from nano to global scales, Atmos. Chem. Phys., 9, 2825–2841, doi:10.5194/acp-9-2825-2009, 2009.

Kulmala, M., Asmi, A., Lappalainen, H. K., Baltensperger, U., Brenguier, J.-L., Facchini, M. C., Hansson, H.-C., Hov, Ø., O'Dowd, C. D., Pöschl, U., Wiedensohler, A., Boers, R., Boucher, O., de Leeuw, G., Denier van der Gon, H. A. C., Feichter, J., Krejci, R., Laj, P., Lihavainen, H., Lohmann, U., McFiggans, G., Mentel, T., Pilinis, C., Riipinen, I., Schulz, M., Stohl, A., Swietlicki, E., Vignati, E., Alves, C., Amann, M., Ammann, M., Arabas, S., Artaxo, P., Baars, H., Beddows, D. C. S., Bergström, R., Beukes, J. P., Bilde, M., Burkhart, J. F., Canonaco, F.,

Clegg, S. L., Coe, H., Crumeyrolle, S., D'Anna, B., Decesari, S., Gilardoni, S., Fischer, M., Fjaeraa, A. M., Fountoukis, C., George, C., Gomes, L., Halloran, P., Hamburger, T., Harrison, R. M., Herrmann, H., Hoffmann, T., Hoose, C., Hu, M., Hyvärinen, A., Hõrrak, U., Iinuma, Y., Iversen, T., Josipovic, M., Kanakidou, M., Kiendler-Scharr, A., Kirkevåg, A., Kiss, G., Klimont, Z., Kolmonen, P., Komppula, M., Kristjánsson, J.-E., Laakso, L., Laaksonen, A., Labonnote, L., Lanz, V. A., Lehtinen, K. E. J., Rizzo, L. V., Makkonen, R., Manninen, H. E., McMeeking, G., Merikanto, J., Minikin, A., Mirme, S., Morgan, W. T., Nemitz, E., O'Donnell, D., Panwar, T. S., Pawlowska, H., Petzold, A., Pienaar, J. J., Pio, C., Plass-Duelmer, C., Prévôt, A. S. H., Pryor, S., Reddington, C. L., Roberts, G., Rosenfeld, D., Schwarz, J., Seland, Ø., Sellegri, K., Shen, X. J., Shiraiwa, M., Siebert, H., Sierau, B., Simpson, D., Sun, J. Y., Topping, D., Tunved, P., Vaattovaara, P., Vakkari, V., Veefkind, J. P., Visschedijk, A., Vuollekoski, H., Vuolo, R., Wehner, B., Wildt, J., Woodward, S., Worsnop, D. R., van Zadelhoff, G.-J., Zardini, A. A., Zhang, K., van Zyl, P. G., Kerminen, V.-M., S Carslaw, K., and Pandis, S. N.: General overview: European Integrated project on Aerosol Cloud Climate and Air Quality interactions (EUCAARI) – integrating aerosol research from nano to global scales, Atmos. Chem. Phys., 11, 13061–13143, doi:10.5194/acp-11-13061-2011, 2011.

Lane, T. E., Donahue, N. M., and Pandis, S. N.: Simulating secondary organic aerosol formation using the volatility basis-set approach in a chemical transport model, Atmos. Environ., 42, 7439–7451, doi:10.1016/j.atmosenv.2008.06.026, 2008.

Langmann, B., Sellegri, K., and Freney, E.: Secondary organic aerosol formation during June 2010 in Central Europe: measurements and modelling studies with a mixed thermodynamic-kinetic approach, Atmos. Chem. Phys., 14, 3831–3842, doi:10.5194/acp-14-3831-2014, 2014.

Li, Y. P., Elbern, H., Lu, K. D., Friese, E., Kiendler-Scharr, A., Mentel, Th. F., Wang, X. S., Wahner, A., and Zhang, Y. H.: Updated aerosol module and its application to simulate secondary organic aerosols during IMPACT campaign May 2008, Atmos. Chem. Phys., 13, 6289–6304, doi:10.5194/acp-13-6289-2013, 2013.

Madronich, S.: The Tropospheric Visible Ultra-violet (TUV) model web page, National Center for Atmospheric Research, Boulder, CO, available at: http://cprm.acd.ucar.edu/Models/TUV/ (last access: 17 December 2015), 2002.

Mensah, A. A., Holzinger, R., Otjes, R., Trimborn, A., Mentel, Th. F., ten Brink, H., Henzing, B., and Kiendler-Scharr, A.: Aerosol chemical composition at Cabauw, The Netherlands as ob-

served in two intensive periods in May 2008 and March 2009, Atmos. Chem. Phys., 12, 4723–4742, doi:10.5194/acp-12-4723-2012, 2012.

Murphy, B. N. and Pandis, S. N.: Simulating the formation of semivolatile primary and secondary organic aerosol in a regional chemical transport model, Environ. Sci. Technol., 43, 4722–4728, 2009.

Murphy, B. N., Donahue, N. M., Fountoukis, C., Dall'Osto, M., O'Dowd, C., Kiendler-Scharr, A., and Pandis, S. N.: Functionalization and fragmentation during ambient organic aerosol aging: application of the 2-D volatility basis set to field studies, Atmos. Chem. Phys., 12, 10797–10816, doi:10.5194/acp-12-10797-2012, 2012.

Nenes, A., Pandis, S. N., and Pilinis, C.: ISORROPIA: a new thermodynamic equilibrium model for multiphase multicomponent inorganic aerosols, Aquat. Geochem., 4, 123–152, 1998.

Pandolfi, M., Querol, X., Alastuey, A., Jimenez, J. L., Jorba, O., Day, D., Ortega, A., Cubison, M. J., Comerón, A., Sicard, M., Mohr, C., Prévôt, A. S. H., Minguillón, M. C., Pey, J., Baldasano, J. M., Burkhart, J. F., Seco, R., Peñuelas, J., Van Drooge, B. L., Artiñano, B., Di Marco, C., Nemitz, E., Schallhart, S., Metzger, A., Hansel, A., Lorente, J., Ng, S., Jayne, J., and Szidat, S.: Effects of sources and meteorology on particulate matter in the Western Mediterranean Basin: an overview of the DAURE campaign, J. Geophys. Res.-Atmos., 119, 4978–5010, doi:10.1002/2013JD021079, 2014.

Passant, N. R.: Speciation of UK emissions of non-methane volatile organic compounds, AEA Technology, Culham, UK, 289, 2002.

Robinson, A. L., Donahue, N. M., Shrivastava, M. K., Weitkamp, E. A., Sage, A. M., Grieshop, A. P., Lane, T. E., Pierce, J. R., and Pandis, S. N.: Rethinking organic aerosols: semivolatile emissions and photochemical aging, Science, 315, 1259–1262, doi:10.1126/science.1133061, 2007.

Shrivastava, M., Fast, J., Easter, R., Gustafson Jr., W. I., Zaveri, R. A., Jimenez, J. L., Saide, P., and Hodzic, A.: Modeling organic aerosols in a megacity: comparison of simple and complex representations of the volatility basis set approach, Atmos. Chem. Phys., 11, 6639–6662, doi:10.5194/acp-11-6639-2011, 2011.

Solazzo, E., Bianconi, R., Pirovano, G., Matthias, V., Vautard, R., Moran, M. D., Appel, K. W., Bessagnet, B., Brandt, J., Christensen, J. H., Chemel, C., Coll, I., Ferreira, J., Forkel, R., Francis, X. V., Grell, G., Grossi, P., Hansen, A. B., Miranda, A. I., Nopmongcol, U., Prank, M., Sartelet, K. N., Schaap, M., Silver, J. D., Sokhi, R. S., Vira, J., Werhahn, J., Wolke, R., Yarwood, G., Zhang, J., Rao, S. T., and Galmarini, S.: Operational model evaluation for par-

ticulate matter in Europe and North America in the context of AQMEII, Atmos. Environ., 53, 75–92, doi:10.1016/j.atmosenv.2012.02.045, 2012.

Starcrest Consulting Group, LLC.: Port-Wide Baseline Air Emissions Inventory, Prepared for the Port of Los Angeles, California, USA, 2004.

Steinbacher, M., Zellweger, C., Schwarzenbach, B., Bugmann, S., Buchmann, B., Ordóñez, C., Prevot, A. S. H., and Hueglin, C.: Nitrogen oxides measurements at rural sites in Switzerland: bias of conventional measurement techniques, J. Geophys. Res., 112, D11307, doi:10.1029/2006JD007971, 2007.

Strader, R., Lurmann, F., and Pandis, S. N.: Evaluation of secondary organic aerosol formation in winter, Atmos. Environ., 33, 4849–4863, 1999.

Tsigaridis, K., Daskalakis, N., Kanakidou, M., Adams, P. J., Artaxo, P., Bahadur, R., Balkanski, Y., Bauer, S. E., Bellouin, N., Benedetti, A., Bergman, T., Berntsen, T. K., Beukes, J. P., Bian, H., Carslaw, K. S., Chin, M., Curci, G., Diehl, T., Easter, R. C., Ghan, S. J., Gong, S. L., Hodzic, A., Hoyle, C. R., Iversen, T., Jathar, S., Jimenez, J. L., Kaiser, J. W., Kirkevåg, A., Koch, D., Kokkola, H., Lee, Y. H, Lin, G., Liu, X., Luo, G., Ma, X., Mann, G. W., Mihalopoulos, N., Morcrette, J.-J., Müller, J.-F., Myhre, G., Myriokefalitakis, S., Ng, N. L., O'Donnell, D., Penner, J. E., Pozzoli, L., Pringle, K. J., Russell, L. M., Schulz, M., Sciare, J., Seland, Ø., Shindell, D. T., Sillman, S., Skeie, R. B., Spracklen, D., Stavrakou, T., Steenrod, S. D., Takemura, T., Tiitta, P., Tilmes, S., Tost, H., van Noije, T., van Zyl, P. G., von Salzen, K., Yu, F., Wang, Z., Wang, Z., Zaveri, R. A., Zhang, H., Zhang, K., Zhang, Q., and Zhang, X.: The AeroCom evaluation and intercomparison of organic aerosol in global models, Atmos. Chem. Phys., 14, 10845–10895, doi:10.5194/acp-14-10845-2014, 2014.

Tsimpidi, A. P., Karydis, V. A., Zavala, M., Lei, W., Molina, L., Ulbrich, I. M., Jimenez, J. L., and Pandis, S. N.: Evaluation of the volatility basis-set approach for the simulation of organic aerosol formation in the Mexico City metropolitan area, Atmos. Chem. Phys., 10, 525–546, doi:10.5194/acp-10-525-2010, 2010.

Tørseth, K., Aas, W., Breivik, K., Fjæraa, A. M., Fiebig, M., Hjellbrekke, A. G., Lund Myhre, C., Solberg, S., and Yttri, K. E.: Introduction to the European Monitoring and Evaluation Programme (EMEP) and observed atmospheric composition change during 1972–2009, Atmos. Chem. Phys., 12, 5447–5481, doi:10.5194/acp-12-5447-2012, 2012.

Vestreng, V., Myhre, G., Fagerli, H., Reis, S., and Tarrasón, L.: Twenty-five years of continuous sulphur dioxide emission reduction in Europe, Atmos. Chem. Phys., 7, 3663–3681, doi:10.5194/acp-7-3663-2007, 2007.

WHO: Burden of disease from Ambient Air Pollution for 2012 – Summary of results, Geneva, Switzerland, 2014.

Yarwood, G., Rao, S., Yocke, M., and Whitten, G. Z.: Updates to the Carbon Bond Chemical Mechanism: CB05, Yocke & Company, Novato, CA, USA, 94945RT-04-00675, 2005.

Zhang, L., Brook, J. R., and Vet, R.: A revised parameterization for gaseous dry deposition in air-quality models, Atmos. Chem. Phys., 3, 2067–2082, doi:10.5194/acp-3-2067-2003, 2003.

Zhang, Q. J., Beekmann, M., Drewnick, F., Freutel, F., Schneider, J., Crippa, M., Prevot, A. S. H., Baltensperger, U., Poulain, L., Wiedensohler, A., Sciare, J., Gros, V., Borbon, A., Colomb, A., Michoud, V., Doussin, J.-F., Denier van der Gon, H. A. C., Haeffelin, M., Dupont, J.-C., Siour, G., Petetin, H., Bessagnet, B., Pandis, S. N., Hodzic, A., Sanchez, O., Honoré, C., and Perrussel, O.: Formation of organic aerosol in the Paris region during the MEGAPOLI summer campaign: evaluation of the volatility-basis-set approach within the CHIMERE model, Atmos. Chem. Phys., 13, 5767–5790, doi:10.5194/acp-13-5767-2013, 2013.

Title Page

Abstract   Introduction

Conclusions   References

Tables   Figures

◄   ►

◄   ►

Back   Close

Full Screen / Esc

Printer-friendly Version

Interactive Discussion

Table 1. Volatility distributions used for different scenarios.

Scenarios	POA emission sources	Emission fraction for volatility bin with C^* of				
		0	1	10	100	1000
Scenario1 (non-volatile CAMxv5.40)	HOA-like	1.00	–	–	–	–
	BBOA-like	1.00				
Scenario2 (Robinson et al., 2007)	HOA-like	0.09	0.09	0.14	0.18	0.5
	BBOA-like	0.09	0.09	0.14	0.18	0.5
Scenario3 (Tsimpidi et al., 2010 and Shrivastava et al., 2011)	HOA-like	0.40	0.26	0.40	0.51	1.43
	BBOA-like	0.27	0.27	0.42	0.54	1.50

Discussion Paper | Discussion Paper | Discussion Paper | Discussion Paper

ACPD

15, 35645–35691, 2015

European air quality modelled by CAMx

G. Ciarelli et al.

Title Page

Abstract   Introduction

Conclusions   References

Tables   Figures

◄   ►

◄   ►

Back   Close

Full Screen / Esc

Printer-friendly Version

Interactive Discussion

Table 2. Model gas phase and PM$_{2.5}$ performance for the EDIII field campaigns (base case S3).

Species	Number of sites	Observed mean (ppb) (μg m^{-3} for PM$_{2.5}$)	Modelled mean (ppb) (μg m^{-3} for PM$_{2.5}$)	MB (ppb) (μg m^{-3} for PM$_{2.5}$)	ME (ppb) (μg m^{-3} for PM$_{2.5}$)	MFB [–]	MFE [–]
			Jun 2006				
CO	36	192.0	158.0	−34.20	80.70	−0.12	0.36
NO$_2$	320	4.1	2.3	−1.87	2.24	−0.54	0.68
O$_3$	460	42.3	51.2	8.93	10.80	0.21	0.24
PM$_{2.5}$	48	12.0	11.7	−0.30	4.46	−0.07	0.39
SO$_2$	263	1.0	1.2	0.20	0.74	0.14	0.67
			Jan–Feb 2007				
CO	45	248.0	191.0	−57.80	107.00	−0.11	0.37
NO$_2$	337	6.5	4.4	−2.17	3.16	−0.28	0.57
O$_3$	455	23.5	35.8	12.30	12.60	0.48	0.49
PM$_{2.5}$	56	11.7	12.8	1.04	6.06	−0.04	0.56
SO$_2$	271	1.3	1.7	0.38	1.09	0.36	0.75
			Sep–Oct 2008				
CO	53	208.0	136.0	−72.00	91.40	−0.31	0.48
NO$_2$	370	5.3	3.7	−1.67	2.50	−0.28	0.56
O$_3$	465	24.3	32.5	8.17	9.58	0.32	0.37
PM$_{2.5}$	90	13.0	14.1	1.03	5.69	< 0.01	0.46
SO$_2$	256	0.9	1.1	0.20	0.76	0.25	0.74
			Feb–Mar 2009				
CO	57	262.0	170.0	−91.60	119.00	−0.26	0.48
NO$_2$	380	6.0	3.9	−2.03	2.78	−0.33	0.56
O$_3$	488	32.7	33.0	0.22	7.14	0.02	0.23
PM$_{2.5}$	110	15.1	13.0	−2.13	6.37	−0.13	0.50
SO$_2$	257	1.0	1.3	0.31	0.86	0.23	0.76

Title Page

Abstract | Introduction

Conclusions | References

Tables | Figures

|◄ | ►|

◄ | ►

Back | Close

Full Screen / Esc

Table 3. Statistical analysis of nitrate, ammonium, sulfate and organic aerosol in base case (S3) for February–March 2009 at different AMS sites.

Site	Mean observed ($\mu g\,m^{-3}$)	Mean modelled ($\mu g\,m^{-3}$)	MB $\mu g\,m^{-3}$	ME $\mu g\,m^{-3}$	MFB [–]	MFE [–]
NO_3^-						
Barcelona	3.6	5.8	2.19	3.98	0.35	0.98
Cabauw	2.2	6.7	4.49	4.58	0.85	1.01
Chilbolton	2.7	4.0	1.33	2.21	0.02	0.76
Helsinki	1.0	1.9	0.93	1.30	0.29	0.92
Hyytiälä	0.2	1.0	0.75	0.83	0.21	1.09
Mace Head	0.6	1.7	1.11	1.12	0.14	0.70
Melpitz	3.1	4.3	1.25	2.41	0.35	0.71
Montseny	3.1	5.9	2.83	4.31	0.38	1.00
Payerne	3.9	5.7	1.81	2.83	0.34	0.61
Puy de Dôme	0.9	2.7	1.81	2.17	1.13	1.30
Vavihill	2.8	3.7	0.89	2.17	0.14	0.78
NH_4^-						
Barcelona	1.6	2.5	0.92	1.41	0.42	0.71
Cabauw	1.0	2.7	1.73	1.75	0.95	0.97
Chilbolton	1.3	2.0	0.68	1.02	0.39	0.61
Helsinki	0.8	1.3	0.52	0.59	0.51	0.60
Hyytiälä	0.4	0.8	0.43	0.48	0.55	0.70
Melpitz	1.4	2.1	0.72	1.11	0.45	0.69
Montseny	1.7	2.6	0.92	1.58	0.39	0.74
Payerne	1.7	2.5	0.80	1.15	0.36	0.56
Puy de Dôme	0.7	1.2	0.51	0.87	0.83	1.07
Vavihill	1.6	1.9	0.38	0.90	0.17	0.56
SO_4^{2-}						
Barcelona	2.7	2.3	−0.44	1.25	−0.19	0.48
Cabauw	1.0	2.1	1.13	1.34	0.73	0.85
Chilbolton	1.3	2.2	0.91	1.33	0.45	0.70
Helsinki	2.4	2.2	−0.24	0.92	−0.04	0.43
Hyytiälä	1.4	1.7	0.26	0.73	0.09	0.58
Mace Head	0.4	1.2	0.83	0.89	1.04	1.12
Melpitz	1.1	2.2	1.15	1.40	0.54	0.76
Montseny	1.4	2.3	0.97	1.19	0.55	0.64
Payerne	1.1	2.1	1.06	1.16	0.62	0.70
Puy de Dôme	0.4	1.1	0.77	0.82	1.14	1.19
Vavihill	1.6	2.3	0.73	1.05	0.18	0.54
OA						
Barcelona	8.2	3.1	−5.11	5.15	−0.80	0.82
Cabauw	1.2	1.1	−0.14	0.53	−0.13	0.50
Chilbolton	2.4	0.7	−1.70	1.70	−1.09	1.10
Helsinki	2.7	2.9	0.26	1.64	0.08	0.62
Hyytiälä	1.3	1.0	−0.28	0.52	−0.48	0.60
Mace Head	0.8	0.4	−0.38	0.43	−0.29	0.70
Melpitz	1.5	0.5	−0.95	0.98	−0.94	0.97
Montseny	3.1	3.9	0.88	1.88	0.31	0.57
Payerne	4.1	1.8	−2.33	2.43	−0.85	0.90
Puy de Dôme	0.6	1.4	0.78	0.96	0.68	0.91
Vavihill	3.9	1.4	−2.53	2.53	−1.04	1.04

Table 4. Statistical analysis of OA for S1, S2 and S3 scenarios for the 11 AMS sites for February–March 2009.

Scenario	Mean observed OA ($\mu g\,m^{-3}$)	Mean modelled OA ($\mu g\,m^3$)	MB ($\mu g\,m^{-3}$)	ME ($\mu g\,m^{-3}$)	MFB [–]	MFE [–]
S1	2.96	1.18	−1.78	2.04	−0.66	0.88
S2	2.96	0.67	−2.29	2.35	−1.08	1.19
S3 (base case)	2.96	1.73	−1.23	1.83	−0.47	0.79

Table 5. Statistical analysis of OA for S3, S4 and S5 scenarios for the 11 AMS sites for February–March 2009.

Scenario	Mean observed OA ($\mu g\,m^{-3}$)	Mean modelled OA ($\mu g\,m^3$)	MB ($\mu g\,m^{-3}$)	ME ($\mu g\,m^{-3}$)	MFB [–]	MFE [–]
S3 (base case)	2.96	1.73	−1.23	1.83	−0.47	0.79
S4	2.96	1.78	−1.17	1.82	−0.46	0.78
S5	2.96	2.84	−0.11	1.91	−0.12	0.69
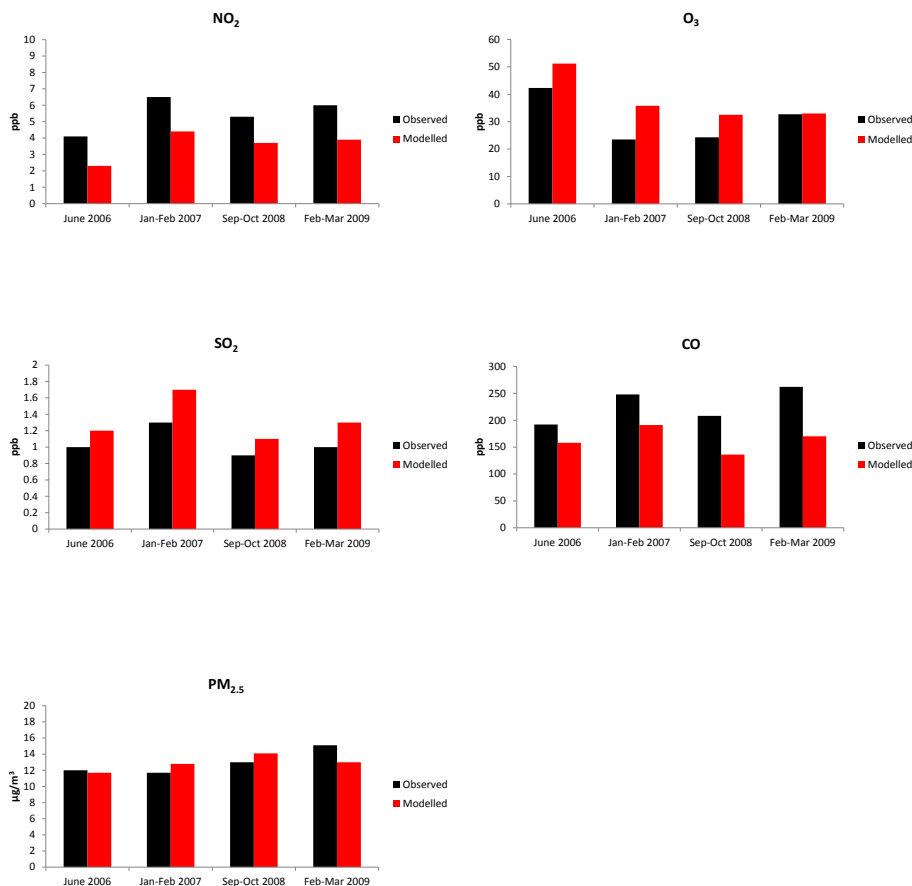
Figure 1. Observed and modelled means for NO_2, O_3, SO_2, CO and $PM_{2.5}$ for Airbase rural background sites with at least 80 % of data available for June 2006, January–February 2007, September–October 2008 and February–March 2009. Number of sites is reported in Table 2.
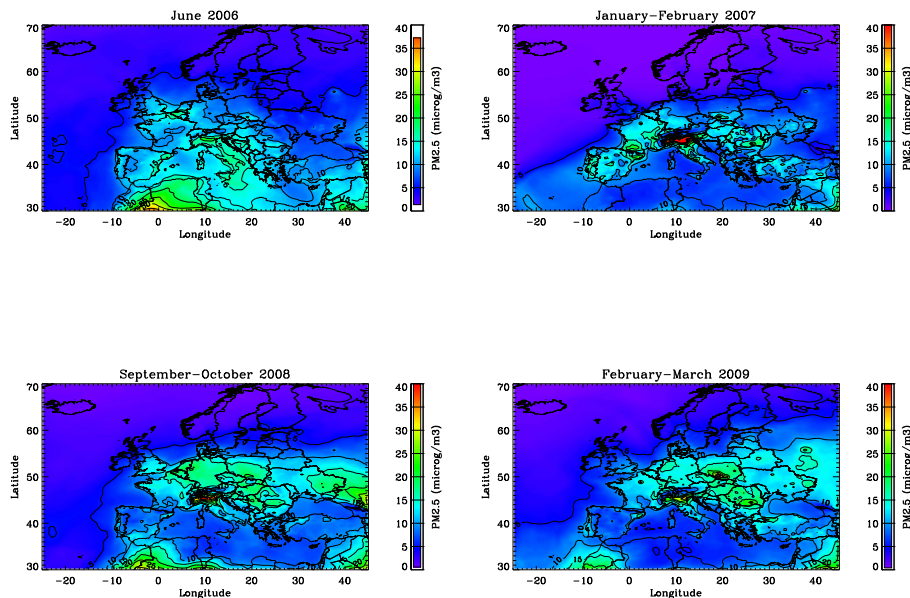
Figure 2. Modelled average PM$_{2.5}$ concentrations for June 2006, January–February 2007, September–October 2008 and February–March 2009 (top to bottom) based on the base case (S3). Note that the color scale was limited to maximum of 40 µg m^{-3} to facilitate comparison of the panels.
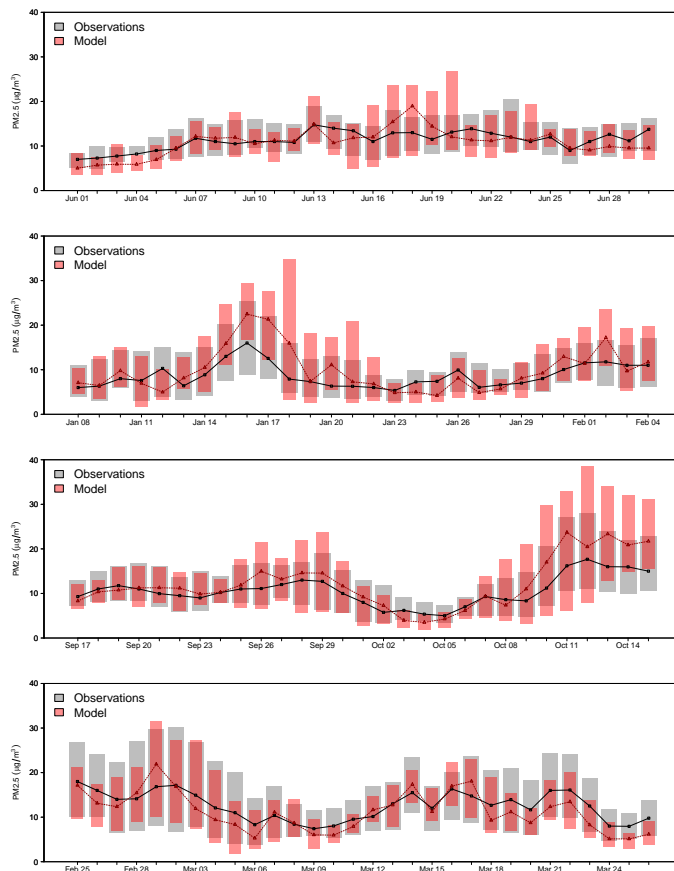
Figure 3. Comparison of modelled (red) and measured (grey) PM$_{2.5}$ concentrations at AirBase rural background sites. The extent of the bars indicates the 25th and 75th percentile. The black and red lines are observed and modelled median, respectively. The numbers of sites are 48, 58, 90, and 110 from top to down. Based on base case (S3).

Title Page

Abstract | Introduction

Conclusions | References

Tables | Figures

|◄ | ►|

◄ | ►

Back | Close

Full Screen / Esc

Printer-friendly Version

Interactive Discussion
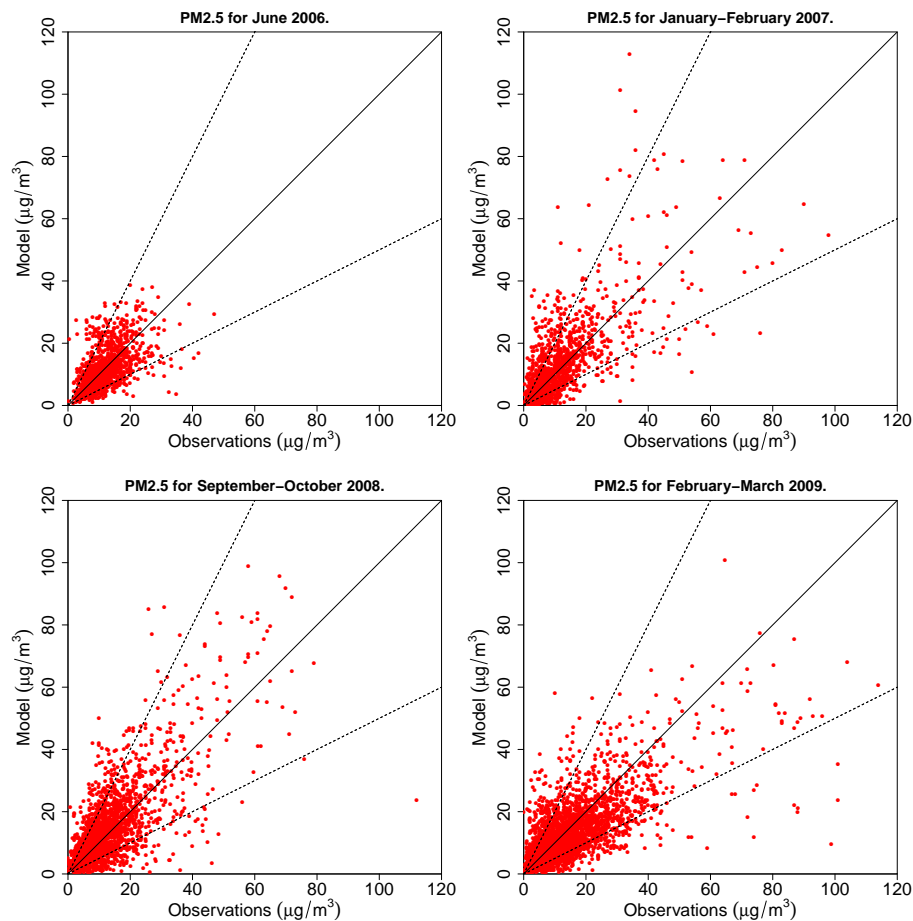
Figure 4. Daily average scatter plots for PM$_{2.5}$ at AirBase rural background sites. Solid lines indicate the 1 : 1 line. Dotted lines are the 1 : 2 and 2 : 1 lines. Based on base case (S3).
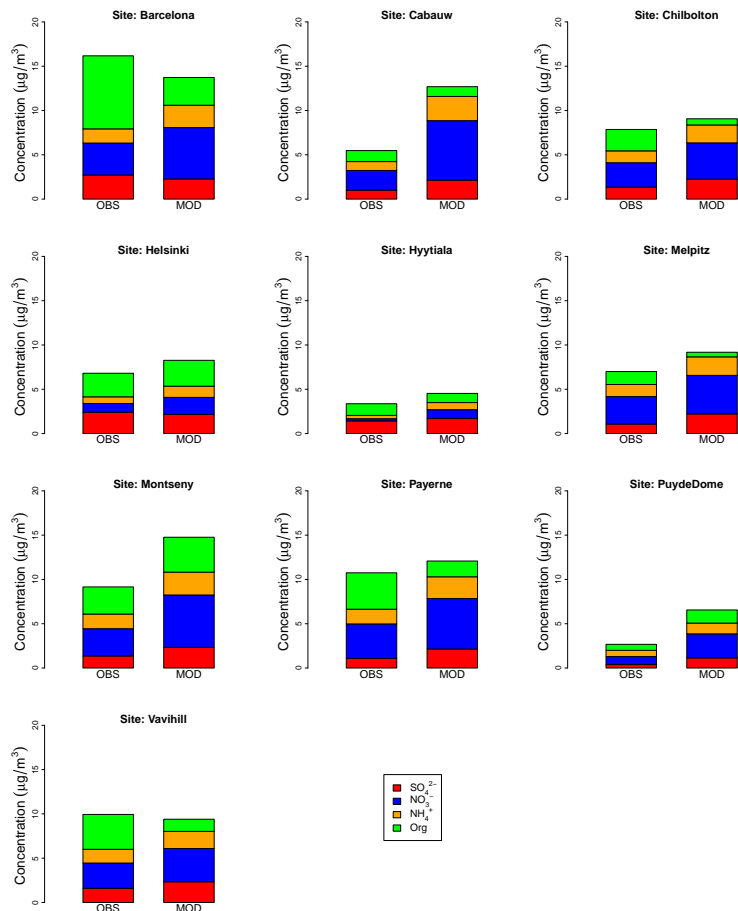
Figure 5. Comparison of observed (OBS) non-refractory PM$_1$ and modelled (MOD) non-refractory PM$_{2.5}$ at 10 AMS sites in Europe. Mace head is reported only in Table 3 since the ammonium component is not available.

Title Page

Abstract | Introduction

Conclusions | References

Tables | Figures

◄ | ►

◄ | ►

Back | Close

Full Screen / Esc

Printer-friendly Version

Interactive Discussion
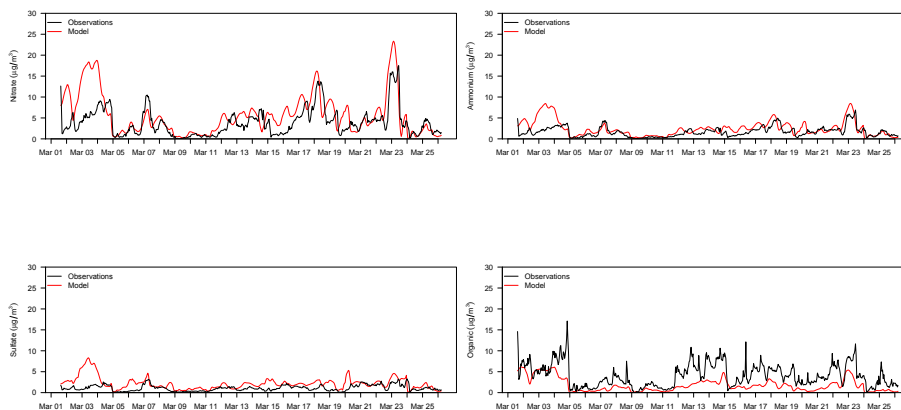
Figure 6. Comparison of observed and modelled nitrate, ammonium, sulfate and organic aerosol at Payerne for March 2009.
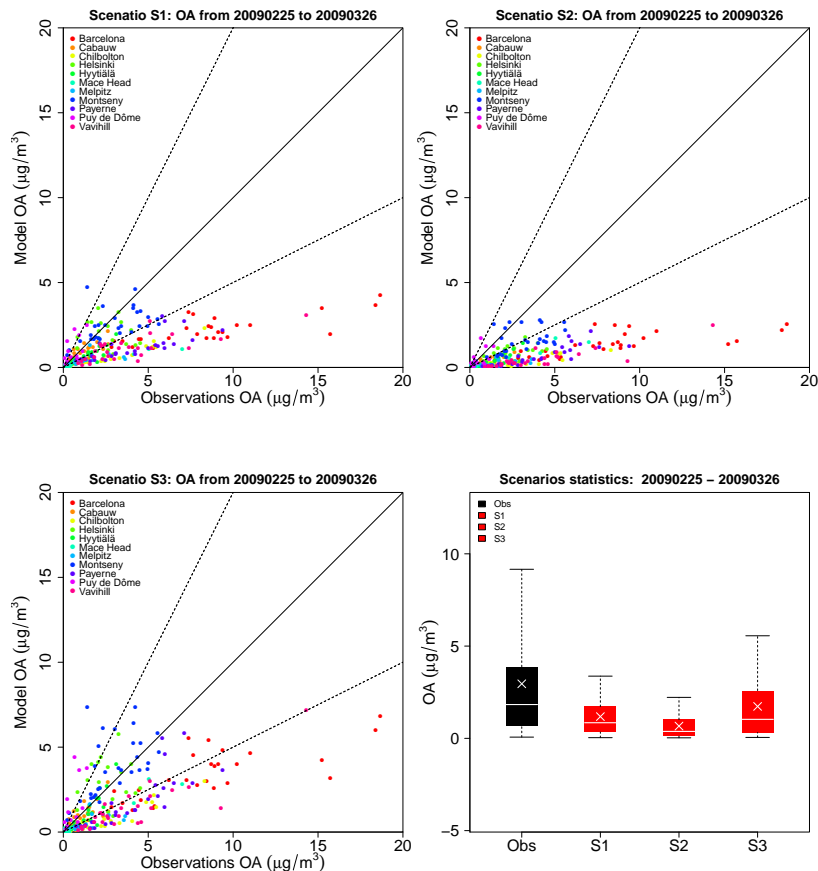
Figure 7. OA daily average scatter plots for S1, S2 and S3 scenarios for February–March 2009 for stations in Table 3. Solid lines indicate the 1 : 1 line. Dotted lines are the 1 : 2 and 2 : 1 lines. Boxplots indicate medians, 5th, 25th, 75th and 95th quantiles for observations (black) and sensitivity tests (red). The crosses represent the arithmetic means.

Title Page

Abstract | Introduction

Conclusions | References

Tables | Figures

|◄ | ►|

◄ | ►

Back | Close

Full Screen / Esc

Printer-friendly Version

Interactive Discussion
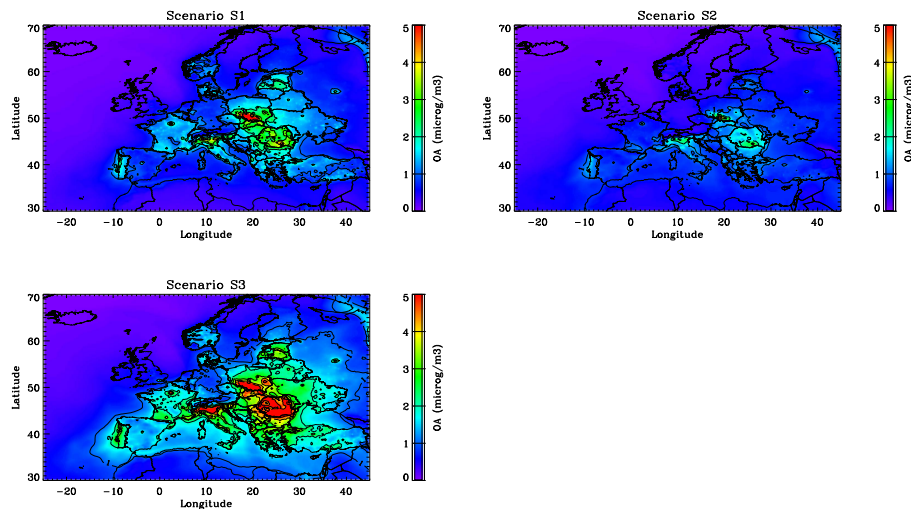
Figure 8. Predicted OA concentrations over Europe for the S1, S2 and S3 scenario in February–March 2009. Note that the color scale was limited to maximum of $5\,\mu g\,m^{-3}$ to facilitate comparison of the panels.

Full Screen / Esc

Printer-friendly Version

Interactive Discussion
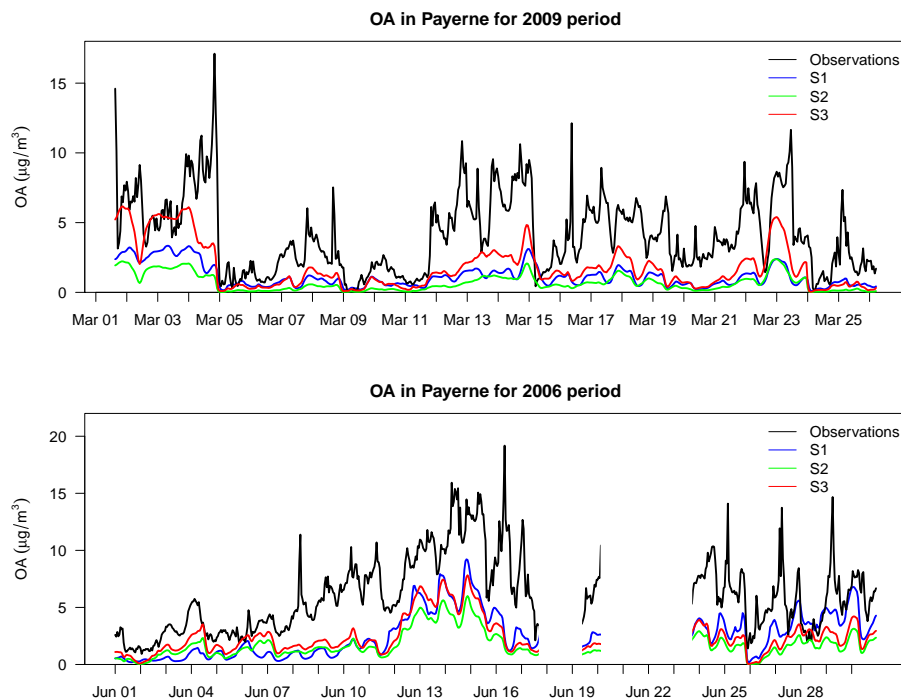
Figure 9. Predicted and observed total OA for scenarios S1, S2 and S3 in March 2009 (upper panel) and June 2006 (lower panel) at Payerne.
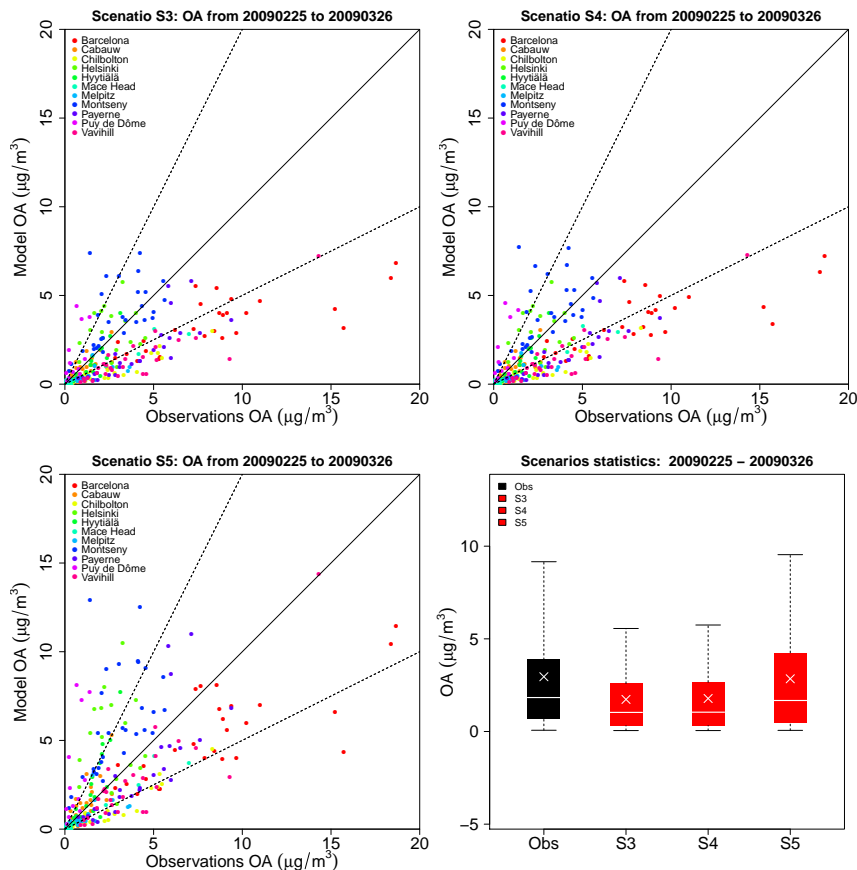
Figure 10. OA daily average scatter plots for S3, S4 and S5 scenarios for February–March 2009 for stations in Table 3. Solid lines indicate the 1 : 1 line. Dotted lines are the 1 : 2 and 2 : 1 lines. Boxplots indicate medians, 5th, 25th, 75th and 95th quantiles for observations (black) and sensitivity tests (red). The crosses represent the arithmetic means.

Title Page

Abstract | Introduction

Conclusions | References

Tables | Figures

|◄ | ►|

◄ | ►

Back | Close

Full Screen / Esc

Printer-friendly Version

Interactive Discussion

OA in Payerne for 2009 period

OA in Payerne for 2006 period
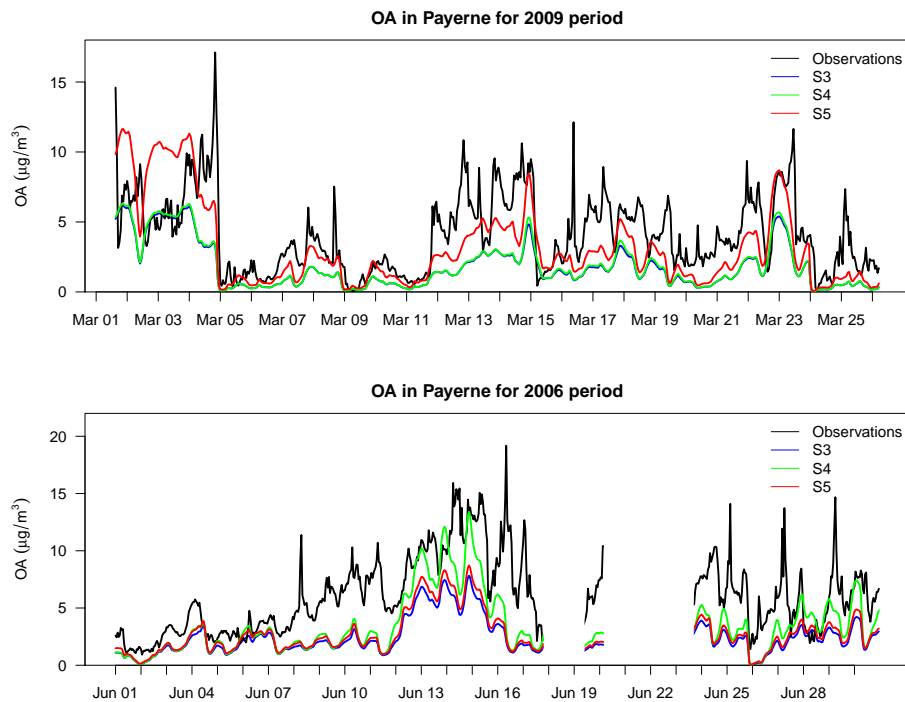
Figure 11. Predicted and observed total OA for scenarios S3, S4 and S5 in March 2009 (upper panel) and June 2006 (lower panel) at Payerne.